Magnetars from Neutron Star–White Dwarf Mergers: Application to Fast Radio Bursts

Shu-Qing Zhong[1,2] and Zi-Gao Dai[1,2]

[1] School of Astronomy and Space Science, Nanjing University, Nanjing 210093, People's Republic of China; sqzhong@hotmail.com, dzg@nju.edu.cn
[2] Key laboratory of Modern Astronomy and Astrophysics (Nanjing University), Ministry of Education, Nanjing 210093, People's Republic of China

Abstract

It is widely believed that magnetars could be born in core-collapse supernovae (SNe), binary neutron star (BNS) or binary white dwarf (BWD) mergers, or accretion-induced collapse (AIC) of white dwarfs. In this paper, we investigate whether magnetars could also be produced from neutron star–white dwarf (NSWD) mergers, motivated by FRB 180924-like fast radio bursts (FRBs) possibly from magnetars born in BNS/BWD/AIC channels suggested by Margalit et al. (2019). By a preliminary calculation, we find that NSWD mergers with unstable mass transfer could result in the NS acquiring an ultra-strong magnetic field via the dynamo mechanism due to differential rotation and convection or possibly via the magnetic flux conservation scenario of a fossil field. If NSWD mergers can indeed create magnetars, then such objects could produce at least a subset of FRB 180924-like FRBs within the framework of flaring magnetars, since the ejecta, local environments, and host galaxies of the final remnants from NSWD mergers resemble those of BNS/BWD/AIC channels. This NSWD channel is also able to well explain both the observational properties of FRB 180924-like and FRB 180916.J0158+65-like FRBs within a large range in local environments and host galaxies.

1. Introduction

Fast radio bursts (FRBs) have remained an extragalactic enigma so far (Katz 2018; Popov et al. 2018; Cordes & Chatterjee 2019; Petroff et al. 2019) since they were discovered by Lorimer et al. (2007), Keane et al. (2012), and Thornton et al. (2013). They are millisecond-duration coherent radio pulses with average upper limits of the peak luminosity $L_p \sim 1 \times 10^{42}$–$8 \times 10^{44}\,\mathrm{erg\,s^{-1}}$ and energy $E \sim 7 \times 10^{39}$–$2 \times 10^{42}\,\mathrm{erg}$ (Zhang 2018), characterized by a single peak mainly or multiple peaks rarely (Champion et al. 2016; Farah et al. 2018; Prochaska et al. 2019), phenomenally divided into repeating bursts (Spitler et al. 2016; CHIME/FRB Collaboration et al. 2019a, 2019b, 2020; Kumar et al. 2019) and nonrepeating bursts. To date, over 100 FRBs have been reported in the literature and collected in the FRB Catalogue[3] (Petroff et al. 2016). Meanwhile, to explain this radio phenomena, dozens of progenitor models involved in compact objects have been proposed (Kashiyama et al. 2013; Falcke & Rezzolla 2014; Lyubarsky 2014; Zhang 2014, 2016, 2017; Geng & Huang 2015; Dai et al. 2016; Gu et al. 2016; Lyutikov et al. 2016; Murase et al. 2016; Wang et al. 2016; Beloborodov 2017, 2019; Metzger et al. 2017, 2019; Deng et al. 2018; Margalit & Metzger 2018), accounting for nonrepeating and/or repeating FRBs. A full model list can refer to Platts et al. (2019).[4]

One interesting group of models relevant to a young flaring magnetar with single or clustered flares have been proposed to give rise to nonrepeating or repeating bursts, respectively (Lyubarsky 2014; Katz 2016; Beloborodov 2017, 2019; Kumar et al. 2017; Metzger et al. 2017, 2019; Lu & Kumar 2018). One of them has been developed to successfully explain nearly all observational properties of FRBs such as polarization, rotation measure (RM; Michilli et al. 2018), frequency downward drift (Hessels et al. 2019), persistent radio source and optical

counterpart (Chatterjee et al. 2017; Tendulkar et al. 2017), circumburst dispersion measure (DM), and the "dark periods" between bursts and clustered burst arrival times appearing in FRB 121102 and its hosted low metallicity dwarf star-forming galaxy and its surrounding dense, highly magnetized, and dynamic plasma environment (Chatterjee et al. 2017; Tendulkar et al. 2017) within the framework of synchrotron maser emission from decelerating relativistic blast waves produced by flare ejecta from young magnetars (Metzger et al. 2019). In this framework, repeating FRBs similar to FRB 121102 arise from young and very active millisecond magnetars quite possibly connected with superluminous supernovae (SLSNe) and long-duration gamma-ray bursts (LGRBs; Metzger et al. 2017). Therefore, young magnetars giving rise to FRB 121102-like FRBs might be formed during the core-collapse of massive stars associated with SLSNe or LGRBs (SLSNe/LGRBs channels).

On the other hand, young millisecond magnetars could also be born in binary neutron star (BNS) mergers (Rosswog et al. 2003; Price & Rosswog 2006; Giacomazzo & Perna 2013), binary white dwarf (BWD) mergers (King et al. 2001; Yoon et al. 2007; Schwab et al. 2016), or accretion-induced collapse (AIC) of white dwarfs (WDs; Nomoto & Kondo 1991; Tauris et al. 2013; Schwab et al. 2015). These magnetars could produce FRBs analogous to FRB 180924 (Bannister et al. 2019), as suggested by Margalit et al. (2019). Compared with FRBs created from magnetars born in SLSNe/LGRBs channels, the FRBs produced from magnetars born in BNS/BWD/AIC channels could have distinct observational properties. Just like FRBs 180924 and 190523 (Ravi et al. 2019), likely as well as FRB 181112 (Prochaska et al. 2019), they host an old massive galaxy with a relatively low rate of star formation and relatively high metallicity, lie in a large spatially offset location relative to the central containment region of the galaxy, and have low DM and RM contributions from the host galaxy and no bright persistent radio source (Bannister et al. 2019; Ravi et al. 2019). If this is the case, FRBs could be divided into two populations: FRB 121102-

---

[3] http://www.frbcat.org
[4] http://frbtheorycat.org

like bursts stem from young magnetars born in SLSNe/LGRBs channels, while FRB 180924-like cases come from those young magnetars born in BNS/BWD/AIC channels. Additionally, most FRB 180924-like bursts should also be repeating in the flaring magnetar framework due to the event rate comparison between magnetars and total FRB events (Nicholl et al. 2017; Margalit et al. 2019; Ravi 2019), which is supported by FRB 171019 followed by faint bursts (Kumar et al. 2019).

In this paper, we investigate whether or not FRB 180924-like bursts are also likely to be generated by magnetars born in an alternative possible channel: neutron star–white dwarf (NSWD) mergers. This channel has also been briefly mentioned and/or discussed by Liu (2018, 2020), Khokhriakova & Popov (2019), and Beloborodov (2019) previously. To answer this question, we need to study (1) whether this channel can form magnetars or not, and (2) if it can, whether the formed magnetars can account for the observations of FRB 180924-like bursts in the flaring magnetar framework. If this channel can indeed form magnetars, it could increase the magnetar event rate to some extent and contribute to at least a subset of FRBs similar to FRBs 180924, 190523, 181112, and even 180916.J0158+65. In the following, we organize the structure of the paper: Section 2 introduces the possibility and speculation that NSWD mergers could form magnetars; whether or not the NSWD channel can explain the observations of FRB 180924-like cases is discussed in Section 3; and a summary and discussion are presented in Section 4.

2. Magnetars from NSWD Mergers

The explosive outcomes of NSWD mergers have been explored in the literature (Metzger 2012; Margalit & Metzger 2016, 2017; Zenati et al. 2019, 2020; Fernández et al. 2019), but the final remnants of these events have been little investigated (see Paschalidis et al. 2011a, 2011b; Margalit & Metzger 2016). Generally, there are two evolutionary pathways for NSWD binaries, which depend on the critical mass ratio $q_{crit} = M_{WD,crit}/M_{NS}$, where $M_{WD,crit}$ is the critical WD mass and M_{NS} is the NS mass. The first pathway is that the WD fills its Roche lobe and its matter undergoes stable mass transfer to the NS if $q < q_{crit}$, evolving into an ultra-compact X-ray binary. The second pathway is that the WD is tidally disrupted by the NS via unstable mass transfer on a rather short dynamical timescale for $q > q_{crit}$, leading to an NSWD merger (Hjellming & Webbink 1987; Hurley et al. 2002). The critical mass ratio is related to the critical WD mass $M_{WD,crit}$, which is found to be $M_{WD,crit} = 0.37 M_\odot$ (van Haaften et al. 2012) or $M_{WD,crit} = 0.2 M_\odot$ (Bobrick et al. 2017). Thus an NSWD merger with $q > q_{crit}$ is in the case of unstable mass transfer. Toonen et al. (2018) pointed out that over 99.9% of semidetached NSWD systems would merge when $M_{WD,crit} = 0.2 M_\odot$, which indicates that the NSWD merger is a prevalent fate of semidetached NSWD binaries. After an NSWD merger, as shown by Paschalidis et al. (2011a, 2011b), the final remnant both in the inspiraling case and in the head-on case is a spinning Thorne–Zytkow-like object (TZIO; Thorne & Zytkow 1977) surrounded by a massive extended hot disk composed of WD debris without explosive outcomes. Considering the disk winds and nuclear burning, Margalit & Metzger (2016) suggested an NSWD merger likely forms an isolated millisecond pulsar surrounded by an accretion disk at the final stage. Whether or not these final remnants evolve into magnetars has received less attention. How the magnetic fields of the final

remnants evolve remains unknown. Fortunately, it has been suggested that the ultra-strong magnetic fields in magnetars may result from two main scenarios (for a review see Turolla et al. 2015). Although these two scenarios are mainly used for nascent NSs born in SLSNe/LGRBs/BNS/BWD/AIC channels, we guess that they might also be used for "renascent" (magnetic field undergoes amplification) NSs formed in the NSWD channel.

2.1. α–ω Dynamo

The first scenario that we consider is magnetic field amplification by a vigorous dynamo action at the early, highly convective stage of the NSs after mergers: the α dynamo arising from the coupling of convective motions and rotation, and the ω dynamo driven by differential rotation (Duncan & Thompson 1992; Thompson & Duncan 1993). For an NSWD merger, the magnetic field of the NS remnant surrounded by a massive disk may either increase via a dynamo winding-up process (as suggested by Paschalidis et al. 2011b) or decrease through an enhanced ohmic dissipation of accreted matter in the NS′ crust (Konar & Bhattacharya 1997; Urpin & Konenkov 1997; Cumming et al. 2004), somewhat similar to the finding of Sun et al. (2019). We discuss whether this finding is true in the following. Bobrick et al. (2017) showed that NSWD mergers exhibit an exponentially increasing rate of mass transfer during different phase transitions (see Figure 12 in Bobrick et al. 2017), and the NSWD mergers in which the WDs have a higher mass would have a shorter dynamical timescale between the onset of significant mass transfer and the final merger (e.g., only $t_{dyn} \sim 10^{-3}(10^{-5})$ yr $\sim 3 \times 10^4 (3 \times 10^2)$ s for WD mass $\sim 0.75(1.2) M_\odot$, see Figure 13 in Bobrick et al. 2017). However, it is not true that the maximal rate of disk accretion onto the final NS in Figures 11 and 12 of Bobrick et al. (2017) is limited by the Eddington rate since the disk accretion of NS can be highly super-Eddington. If the majority of mass is lost via a disk wind or a possible jet in the mass transfer process and only $0.05 M_\odot$ can be accreted onto the NS, as discussed in Margalit & Metzger (2016) for a WD with mass $0.6 M_\odot$ (close to $0.75 M_\odot$), the NS would accrete the disk material onto its surface with an average rate $\dot{M} \sim 10^{-6} M_\odot\,s^{-1}$ during the short dynamical timescale $\sim 3 \times 10^4$ s. In this case, the accretion of the final NS surrounded by a massive disk may let it differentially and rapidly rotate, as possibly shown by the simulation results of Paschalidis et al. (2011b), even if Paschalidis et al. (2011b) did not take into account explosive outcomes. Moreover, during this short dynamical timescale, transient ohmic dissipation of the final NS could be ignored, see an estimate in Sun et al. (2019) and Equation (9) of Urpin & Konenkov (1997). Therefore, we just need to focus on the magnetic field amplification of the final NS that accretes the WD debris material from the disk during the merger. Owing to the lack of previous studies of the magnetic field evolution of NSWD mergers with unstable and rapid mass transfer, we perform only a preliminary analysis on the α–ω dynamo induced by possible differential rotation and/or convection that can amplify the NS′ magnetic field during the NSWD mergers. In the final paragraph of this subsection, we also discuss the dynamo induced by the magnetorotational instability (MRI; Balbus & Hawley 1998) in the disk that also might contribute to the NS′ magnetic field amplification.

We assume that the final NS with differential rotation induced by accretion has two components: the core and the

shell divided by a boundary at the radius $R_c \cong 0.5R$ (where R is the NS radius), as done by Dai et al. (2006), its accretion can be generally determined by the Alfvén radius

$$
\begin{aligned}
r_m &= (B_s R^3)^{4/7} (GM)^{-1/7} \dot{M}^{-2/7} \\
&= 5.3 \left(\frac{B_s}{10^{12}\,\text{G}} \right)^{4/7} \left(\frac{R}{12\,\text{km}} \right)^{12/7} \left(\frac{M}{1.4\,M_\odot} \right)^{-1/7} \\
&\quad \times \left(\frac{\dot{M}}{10^{-6}\,M_\odot\,\text{s}^{-1}} \right)^{-2/7} \text{km},
\end{aligned}
\tag{1}
$$

where B_s, R, M, and $\dot{M}$ are the surface magnetic dipole field strength, radius, mass, and accretion rate of the NS, respectively, and the corotation radius

$$
\begin{aligned}
r_c &= \left(\frac{GM}{\Omega_s^2} \right)^{1/3} = \left(\frac{GM P_s^2}{4\pi^2} \right)^{1/3} \\
&= 7.8 \times 10^3 \left(\frac{M}{1.4\,M_\odot} \right)^{1/3} \left(\frac{P_s}{10\,\text{s}} \right)^{2/3} \text{km},
\end{aligned}
\tag{2}
$$

where $\Omega_s = 2\pi/P_s$ and P_s are the angular velocity and spin period of the NS′ shell, respectively. One additional key radius is the light cylinder radius,

$$
r_{lc} = c / \Omega_s = 4.8 \times 10^5 \left(\frac{P_s}{10\,\text{s}} \right) \text{km}.
\tag{3}
$$

One expects that in the case of $r_m < r_c < r_{lc}$ for a normal NS in an NSWD merger with $B_s = 10^{12}\,\text{G}$, $M = 1.4\,M_\odot$, $R = 12\,\text{km}$, and $P_s = 10\,\text{s}$, as well as an accretion rate $\dot{M} = 10^{-6}\,M_\odot\,\text{s}^{-1}$, disk material is column-accreted onto the NS′ surface and leads to the NS′ shell to spin up (Frank et al. 1992). Following Piro & Ott (2011) and Dai et al. (2006), the time-dependent angular velocity for the NS′ shell can be solved by

$$
I_s \frac{d\Omega_s}{dt} = N_{acc} - N_{dip} - N_{mag},
\tag{4}
$$

where I_s is the moment of inertia of the shell, and (1) N_{acc} is the accretion torque described by, when $r_m < R$ for a normal NS from Equation (1),

$$
N_{acc} = \left(1 - \frac{\Omega_s}{\Omega_K} \right) (GMR)^{1/2} \dot{M},
\tag{5}
$$

where $\Omega_K = (GM/R^3)^{1/2}$; (2) N_{dip} is the magnetic dipole radiation torque for accreting NSs with $r_m < r_{lc}$, enhanced over the standard dipole torque by a factor of $(r_{lc}/r_m)^2 > 1$ due to the enhanced open magnetic field lines via the compression of the magnetosphere (Parfrey et al. 2016; Metzger et al. 2018), read as

$$
\begin{aligned}
N_{dip} &= \frac{2B_s^2 R^6 \Omega_s^3}{3c^3} \left(\frac{r_{lc}}{r_m} \right)^2 \\
&= \frac{2\Omega_s}{3c} (B_s R^3)^{6/7} (GM)^{2/7} \dot{M}^{4/7};
\end{aligned}
\tag{6}
$$

(3) N_{mag} is the magnetic torque acting between the core and shell, written as

$$
N_{mag} = \frac{2}{3} R_c^3 B_r B_\phi,
\tag{7}
$$

where $B_r = B_s/\epsilon$ (here, ϵ is defined by the ratio of the effective surface dipole field strength to the radial field strength) and B_ϕ are the radial magnetic field component and toroidal field component, respectively. They can be related to each other by

$$
\frac{dB_\phi}{dt} = (\Delta\Omega) B_r \equiv (\Omega_c - \Omega_s) B_r,
\tag{8}
$$

where $\Delta\Omega$ is the differential angular velocity and Ω_c is the NS′ core angular velocity. On the other hand, the time-dependent angular velocity for the NS′ core can be solved by[5]

$$
I_c \frac{d\Omega_c}{dt} = N_{mag},
\tag{9}
$$

where I_c is the moment of inertia of the core. Through Equations (4), (8), and (9), we can solve Ω_s, Ω_c, $\Delta\Omega$, and B_ϕ as illustrated in Figure 1 via numerical calculation, combining Equations (5) and (7). To obtain these results, we have also employed: (1) typical values for a normal NS in an NSWD merger: $M = 1.4\,M_\odot$, $R = 12\,\text{km}$, initial period $P_{s,0} = 10\,\text{s}$, $B_s = 10^{12}\,\text{G}$, $I_s \cong I_c \sim 10^{45}\,\text{g cm}^2$, and $\epsilon = 0.3$ (Dai et al. 2006), as well as an accretion rate $\dot{M} = 10^{-6}\,M_\odot\,\text{s}^{-1}$, such that the term N_{dip} can be ignored in comparison with N_{acc} even if P_s possibly reaches down to its break-up limit $P_{s,min} = 0.96\,\text{ms}$ (Lattimer & Prakash 2004); (2) initial conditions: $\Omega_{s,0} = 2\pi/P_{s,0}$, $\Omega_{c,0} = (1 + A_0)\Omega_{s,0}$ (the initial angular velocity of the core $\Omega_{c,0}$ should be larger than that of the shell $\Omega_{s,0}$ for a normal NS), $A_0 = 10^{-3}$ related to a small residual differential rotation, and $B_{\phi,0} \sim 10^8\,\text{G}$; (3) boundary conditions: $\Omega_s \leqslant \Omega_{s,max} = 6541$ due to $P_{s,min} = 0.96\,\text{ms}$, $\Omega_c < \Omega_{c,max} = c/R_c$, and $B_\phi < B_{\phi,max} = 10^{17}\,\text{G}$ because of the buoyancy effect. From Figure 1, we can acquire the following:

1. The top panel shows that the angular velocity of the shell gradually increases up to its limit at about 200 s and this lasts until the end of the dynamical process. While the angular velocity of the core reverses (rotating in an opposite direction) at about 50 s and its absolute value rapidly rises to a very large value c/R_c[6] at around 1000 s. This is because the toroidal magnetic field B_ϕ reverses, as in the bottom panel. The evolution of the differential angular velocity $\Delta\Omega$ follows the angular velocity of the core.

2. In the bottom panel, the toroidal magnetic field B_ϕ rapidly declines to zero and then reverses before 0.1 s, its absolute value continues going up to the buoyancy limit $10^{17}\,\text{G}$ at about 150 s.

---

5 Please note that the right term of Equation (9) has no negative sign, differing from Equation (3) in Dai et al. (2006) because the magnetic field is amplified via the differential angular velocity resulting from the angular momentum transport of the accreting material onto the NS′ shell rather than the angular momentum loss of the core for an accreting NS system we consider here. The same reason that the right term of Equation (4) in this paper differs from Equation (2) in Dai et al. (2006).

6 The core angular velocity Ω_c that exceeds the break-up limit of the shell is reasonable since this break-up limit should not be that of the core angular velocity. Instead, its limit should be c/R_c.
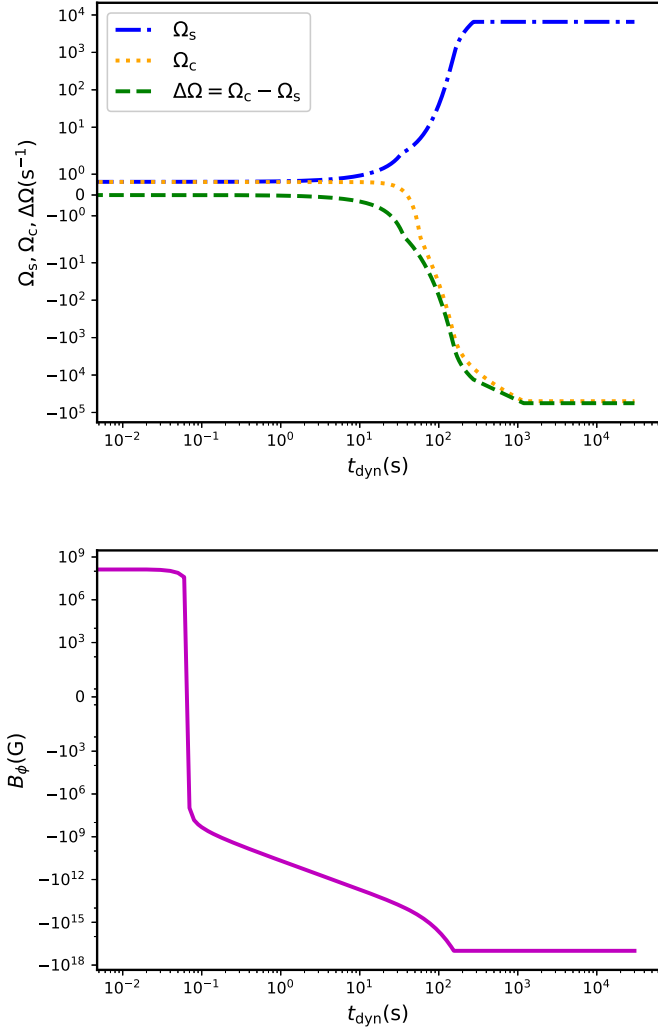
Figure 2. Magnetic dipole radiation evolution of the NS in an NSWD merger during the dynamical timescale.

Figure 1. Evolution of the angular velocities of the shell and the core and the differential angular velocity $\Delta\Omega$ (top panel), and the torodial magnetic field B_ϕ (bottom panel) of the NS in an NSWD merger during the dynamical timescale $t_{dyn} = 3 \times 10^4$ s.

In short, these results manifesting the toroidal magnetic field can be enhanced during the dynamical timescale as long as the initial remnant NS in an NSWD merger has a small residual differential rotation. Additionally, during the field amplification, the spin-down torque N_{dip} responds to the magnetic dipole radiation luminosity

$$L_{dip} = N_{dip}\Omega_s$$
$$= \frac{2\Omega_s^2}{3c}(B_s R^3)^{6/7}(GM)^{2/7}\dot{M}^{4/7}, \quad (10)$$

which follows the evolution of the angular velocity of the shell, as displayed in Figure 2. This Poynting flux could generate a high energy (X-ray/γ-ray) transient lasting hundreds to thousands of seconds via magnetic dissipation with brightness up to $L_{dip,peak} \sim 10^{46}$ erg s^{-1}, which is likely similar to an X-ray transient source named CDF-S XT2 discovered by Xue et al. (2019).

Besides the differential rotation, Duncan & Thompson (1992) and Thompson & Duncan (1993) suggested that a key parameter for the success of α–ω dynamo is the Rossby number R_O relevant to convection (the ratio of the rotation period to the convective
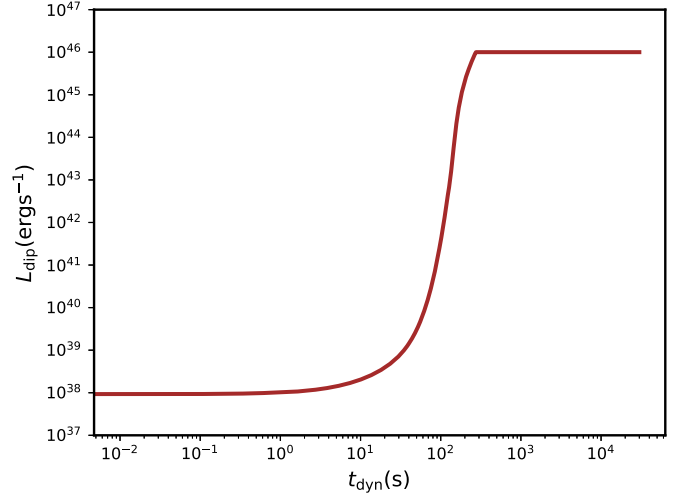
overturn time). An efficient dynamo result needs $R_O \sim 10(P/10 \text{ ms})(F/10^{39} \text{ erg cm}^{-2} \text{ s}^{-1})^{1/3} \leqslant O(1)$ (where F is the entropy-driven convection heat flux). This type of convection usually occurs in a nascent NS left behind the collapse of a massive star, a BNS/BWD merger, or an AIC of a WD with a negative radial entropy gradient from the interior to the outer layers (Thompson & Duncan 1993), but should not occur in the old NS in an NSWD system. However, for the accreting NS in an NSWD merger, its surface should be covered by an accreting envelope with tidal WD debris via magnetically channeled accretion. Under this condition, the accretion flow can produce heat radiation due to the shock heating (see the appendix in Piro & Ott 2011), its temperature is $T_{sh} \sim 8 \times 10^9$ K, if $M = 1.4 M_\odot$, $R = 12$ km, $B_s = 10^{12}$ G, and $\dot{M} = 10^{-6} M_\odot$ s^{-1} are considered (for a detailed derivation please refer to Equation (A1) in Zhong et al. 2019). Therefore, the shock heat cannot escape via neutrino cooling (since a low temperature cannot induce neutrino emission) or photon diffusion (since photons are trapped and advected due to the high accretion rate). Throughout the large and radiatively inefficient accreting envelope, convection may be an important source of outward energy transport (e.g., Quataert & Gruzinov 2000). In this case, the energy flux due to convection in the absence of bulk of motion or angular momentum transport should be from gravitational potential energy flux $F_c \sim GM\dot{M}/(4\pi R^3)$. If the magnetic field of the NS can be enhanced by this convection, the magnetic field could reach its buoyancy value 10^{17} G (please note that $B_c^2/(8\pi) < F_c t_{dyn} \sim [GM\dot{M}/(4\pi R^3)]t_{dyn}$ and thus $B_c < 1.0 \times 10^{20}$ G) under the parameter values $M = 1.4 M_\odot$, $R = 12$ km, $\dot{M} \sim 10^{-6} M_\odot$ s^{-1}, and $t_{dyn} = 3 \times 10^4$ s, although the real circumstance could be more complex.

Differing from the differential rotation and convection processes that occur in the accreting NS of the NSWD merger, an alternative potential process, MRI, possibly occurs in the disk due to the presence of shear, like the disk dynamo in common envelope events for the formation of highly magnetic WDs (Tout et al. 2008; Nordhaus et al. 2011). This process amplifies the disk field, and the field then would be conveyed to the surface of the NS along with the radiatively inefficient magnetically channeled accretion flow. The disk dynamo for WDs in the super-Eddington regime (Nordhaus et al. 2011) should also be suitable for the accretion disk in the NSWD merger. Accordingly, based on Blackman et al. (2001) and

Nordhaus et al. (2011), the mean toroidal field via the MRI in the disk at radius r is estimated by

$$
\begin{aligned}
\bar{B}_\phi &\sim \left(\frac{\dot{M}\Omega_K}{r}\frac{r}{H}\right)^{1/2} \\
&= 6 \times 10^{12}\left(\frac{\dot{M}}{10^{-6}\,M_\odot\,s^{-1}}\right)^{1/2}\left(\frac{M}{1.4\,M_\odot}\right)^{1/4} \\
&\quad \times \left(\frac{r}{12\,\text{km}}\right)^{-5/4}\left(\frac{r/H}{2}\right)^{1/2}\,\text{G}, \quad (11)
\end{aligned}
$$

where $\Omega_K = (GM/r^3)^{1/2}$ is the Keplerian rate the disk orbits, H is the isothermal scale height of the disk. This process can enhance the magnetic field of the NS but could not result in a magnetar-like field.

2.2. Fossil Field

The second scenario that we consider is the magnetic flux conservation–fossil field scenario (Ferrario & Wickramasinghe 2006, 2008), which signifies that the magnetic fields of the NSs and/or the WDs in NSWD binaries should be stronger than normal NSs and/or WDs. Although it is hard to imagine that the progenitors in binary compact stars possess a very strong magnetic field since such strong magnetic fields likely decay on much shorter timescales $\sim 10^{4-5}$ yr (Heyl & Kulkarni 1998; Harding & Lai 2006) than the merger lifetime. However, there may be some speculating clues. For instance, the precursor of GRB 090510 is likely related to a magnetar-like magnetic field ($B > 10^{15}$ G in Troja et al. 2010) of the NS in the progenitors if the precursor stems from the magnetospheric interaction of the NSs. Furthermore, the merger lifetimes can also be much shorter than the inspiral times for a sizable fraction of double NS mergers in some population synthesis models (Belczynski et al. 2002, 2006). After the merger lifetimes, the magnetic fields should have decayed by only a factor of a few, as illuminated in Troja et al. (2010). This result should be suitable at least for a small fraction (a few times 0.1%) of NSWD mergers, since the supernova producing NS precedes the NSWD merger (in which the WD forms before the NS for the majority of NSWD mergers) by less than 100 years, as suggested in Toonen et al. (2018).

Whether or not these scenarios can enhance the magnetic fields of final NSs post NSWD mergers still lacks evidence both in numerical simulations and observations. Accordingly, for the problem of the fate of the remnants' magnetic fields post NSWD mergers, deep and complex exploration and magneto-hydrodynamics simulations for the magnetic field evolution of the remnants are required.

3. Explanations of Observational Properties of FRB 180924-like Bursts

If FRB 180924-like bursts can be produced from magnetars born in NSWD mergers, this NSWD channel should be able to explain all of the observational properties of this FRB population, as well as the event rate, host galaxy and offset, and circumburst environment. Due to the similarities between the NSWD channel and BNS/BWD/AIC channels, we mainly follow Margalit et al. (2019) to analyze and discuss this NSWD channel, which is shown as follows.

(1) *Active Lifetime.* The mass of magnetars formed from NSWD mergers, M_{mag}, could be smaller than or close to the maximal mass

of a nonrotating NS M_{TOV}, given a critical WD mass $M_{\text{WD,crit}} = 0.37\,M_\odot$ or $M_{\text{WD,crit}} = 0.2\,M_\odot$ for unstable mass transfer, and a canonical NS mass $M_{\text{NS}} = 1.4\,M_\odot$. However, these magnetars should have a lower mass than those born in the BNS channel, but likely a higher mass than those born in SLSNe/LGRBs or BWD/AIC channels. Moreover, the mass M_{mag} should also exceed or approach the threshold mass for the onset of direct or modified URCA neutrino cooling (Beloborodov & Li 2016). As pointed out by Margalit et al. (2019), such magnetars may possess sufficiently high central densities (or high temperatures) to activate URCA cooling in their cores. Otherwise, their magnetic dissipation in the core is caused predominately by ambipolar diffusion (Goldreich & Reisenegger 1992; Thompson & Duncan 1996), which is sensitive to the core temperature. Since the core temperature depends on its URCA cooling at early times of magnetar formation, their magnetic activity timescale in the direct URCA cooling (high-mass NS) and modified URCA cooling (normal-mass NS) can be estimated as $t_{\text{mag}} \sim B_{16}^{-1}L_5^{3/2}20$ yr ($700B_{16}^{-1.2}L_5^{1.6}$ yr) for high-mass NS (normal-mass NS; see Equation (33) of Beloborodov & Li 2016). This would correspond to a magnetic energy dissipation with an average luminosity $L_{\text{mag}} \sim 5 \times 10^{40}B_{16}^3$ erg s^{-1} ($10^{39}B_{16}^{3.2}$ erg s^{-1}) for high-mass NS (normal-mass NS; see Equation (2) of Margalit et al. 2019), which is just lower than the peak luminosities of FRBs by two to four orders of magnitude (Zhang 2018).

During the active lifetimes of magnetars, they produce ~ 100 repeating bursts resulting from relativistic blast waves caused by giant flares with luminosity higher than L_{mag} by several orders of magnitude, enough to satisfy the event rate of FRBs (Ravi 2019). Because the active lifetimes are several tens to several hundreds of years, the "dark period" between bursts can average years to several tens of years; there should be different local DMs between bursts even though they stem from the same source. Under this condition, we might regard them as different bursts from different sources rather than repeating bursts from the same source, e.g., two possible cases: FRBs 110220 and 140514 (Piro & Burke-Spolaor 2017), and FRBs 160920 and 170606. Therefore, it is easy to understand that repeating bursts of FRB 180924 have not been detected during a relatively short follow-up observation. This is also supported by the bright FRB 171019 followed by faint bursts (Kumar et al. 2019).

(2) *Burst Transparency.* In the framework of flaring magnetars, bursts can escape only when the surrounding material is free–free transparent for radio frequency $\sim$GHz. Similar to BNS/BWD mergers and AIC, there should also be ejecta surrounding the "renascent" magnetars for the NSWD channel, which may also give rise to observable explosive transients. The ejecta consists of the WD debris disk and the accretion-driven outflow with velocity extending up to $\sim 3 \times 10^4$ km s$^{-1} = 0.1c$, with overall low mass of 0.01–0.1 $M_\odot$ (Zenati et al. 2019). If the free–free optical depth of ejecta for which the temperature and ionization state are governed by photoionization due to spin-down of the "renascent" magnetar, as handled in Margalit et al. (2019), the free–free transparency time could be $t_{\text{ff}} \propto M_{\text{ej}}^{2/5}v_{\text{ej}}^{-1}$ for a fixed ionization fraction (see Equation (18) in Margalit et al. 2018). This result should be comparable to BNS mergers, e.g., $M_{\text{ej}} \sim 0.05\,M_\odot$ and $v_{\text{ej}} \sim 0.2c$ inferred from kilonova emission accompanying GW170817 (Cowperthwaite et al. 2017; Kasen et al. 2017; Villar et al. 2017). Hence, FRBs can pass through the ejecta quickly and escape in just about a few weeks

to months post magnetar formation, compared with $t_{\rm ff} \sim$ 10–100 yr for SLSNe (Margalit et al. 2018).

(3) *Circumburst DM.* The circumburst DM contribution of ejecta to the burst should be akin to that of BNS/BWD/AIC channels, can be calculated by (Margalit et al. 2019)

$$\mathrm{DM_{ej}} \approx \frac{3M_{\rm ej}}{8\pi m_{\rm p}(v_{\rm ej}t)^2} \approx 5 \; \mathrm{pc \; cm^{-3}} M_{\rm ej,-1}\beta_{\rm ej}^{-2} t_{\rm yr}^{-2}, \quad (12)$$

where $M_{\rm ej,-1} = M_{\rm ej}/0.1\,M_\odot$, $\beta_{\rm ej} = v_{\rm ej}/c$ and $t_{\rm yr} = t/1$ yr. For ejecta post NSWD mergers, $M_{\rm ej} \sim 0.01$–$0.1\,M_\odot$ and $v_{\rm ej} \sim 0.1c$, so $\mathrm{DM_{ej}} \sim 50$–500 pc cm^{-3} $t_{\rm yr}^{-2}$. If the radio frequency is transparent after one month, $\mathrm{DM_{ej}}$ would decrease to $5 \times 10^{3-4}$ pc cm^{-3}. For the case of FRB 180924, it has a mean contribution by host galaxy $\mathrm{DM_{host}}$ 30–81 pc cm^{-3} (Bannister et al. 2019). The contribution by its ejecta should be smaller than $\mathrm{DM_{host}}$. If so, FRB 180924 should escape from the ejecta at least one year after the magnetar is born in the NSWD channel, in which time the radio frequency is already transparent. Note that the most repeating FRBs have a nearly invariable DM for long-term observations (Spitler et al. 2016; CHIME/FRB Collaboration et al. 2019a, 2019b, 2020; Kumar et al. 2019) signifying that the DM contribution from their ejecta has declined close to zero several years to several hundreds of years after their magnetar formation.

(4) *RM.* According to Margalit et al. (2018), the maximal contribution to the RM is primarily caused by a nebula in which the cooled electrons and magnetic field injected by magnetar flares in the distant past and confined by the SN ejecta (Beloborodov 2017; Margalit & Metzger 2018). It is given by

$$\mathrm{RM} = \frac{e^3}{2\pi m_{\rm e}^2 c^4} \int n_{\rm e} B_\parallel ds \approx \frac{3e^3}{8\pi^2 m_{\rm e}^2 c^4} \frac{N_{\rm e} B_{\rm n}}{R_{\rm n}^2} \left(\frac{\lambda}{R_{\rm n}}\right)^{1/2}, \quad (13)$$

where the total number of electrons in the nebula

$$N_{\rm e} = \xi E_{\rm mag}, \quad (14)$$

the magnetic field strength in the nebula

$$B_{\rm n} \approx \left(\frac{6\epsilon_B E_{\rm mag} \mathrm{abs}(\alpha - 1)}{R_{\rm n}^3}\right)^{1/2} \left(\frac{t}{t_{\rm mag}}\right)^{(1-\alpha)/2}, \quad (15)$$

and the nebula size $R_{\rm n}$ is set by the outer ejecta radius

$$R_{\rm n} = v_{\rm ej}t, \quad (16)$$

and λ is correlation length-scale of the magnetic field in the nebula, $\epsilon_{\rm B}$ is the ratio of the magnetic energy in the nebula to the magnetic energy injected in relativistic particles over an expansion time t, α is the decay index related to the average magnetic luminosity of the magnetar, and ξ is the average ratio of the number of ejected baryons to the released magnetic energy (Beloborodov 2017). If given $\epsilon_{\rm B} = 0.1$, $\xi = \xi_{\rm max} \approx 4 \times 10^3$ erg^{-1}, $E_{\rm mag} \approx 3 \times 10^{49}$ erg (Beloborodov & Li 2016), $v_{\rm ej} = 0.1c$, $\lambda \sim R_{\rm n}$, and $\alpha = 0$, motivated by magnetic-dissipation-powered FRB models (Margalit et al. 2018) for a magnetar formed from the NSWD channel, its RM is just $\sim$12 rad m^{-2} at the time $t \sim 10^{-1}t_{\rm mag}$, assuming $t_{\rm mag} \sim 100$ yr. Moreover, its RM decreases with time. These results are generally consistent with Margalit et al. (2019) and the RM observation of FRB 180924 (Bannister et al. 2019).

(5) *Persistent Radio Source.* The persistent radio emission arising from the NSWD channel should also be analogous to

that from BNS/BWD/AIC channels, due to the similar properties of their nebula and ejecta. Accordingly, there is no evidence for persistent radio emission in FRB 180924 that can be easily understood using synchrotron radiation in the nebula confined by the ejecta, based on Figure 3 of Margalit et al. (2019).

(6) *Host Galaxy.* Metzger (2012) suggested that NSWD mergers involving pure-He WDs could be related to faint type Ib Ca-rich SNe, which mostly explode in early-type galaxies and old environments (Perets et al. 2010; Kasliwal et al. 2012; Lyman et al. 2013). On the contrary, those mergers relevant to C/O or hybrid C/O/He WDs are likely associated with the transients most similar to SNe Ic (Toonen et al. 2018; Zenati et al. 2019). Moreover, Toonen et al. (2018) showed that only a small fraction are expected to be found in early-type elliptical/ S0 galaxies, while a large subset of NSWD mergers are most likely to be found in late-type, disk, and star-forming galaxies since the delay time distribution peaks at early times (<1–2 Gyr). This is because they argued that hybrid WD mergers are more common than pure He WD mergers. They also obtained that the offsets of NSWD mergers, depending on the stellar density of host galaxies, could range from small offsets due to a low escape velocity for those in dwarf galaxies to very large offsets of up to a few hundred kiloparsecs for those including NS natal kicks. However, it is still possible that some Ca-rich transients originate from He WD mergers, while more massive NSWD mergers give rise to some kind of fast-evolving Ic-like transients (Margalit & Metzger 2016; Fernández et al. 2019). Therefore, we can see that the host galaxies of NSWD mergers are in a large range. In this case, there should be a subset of galaxies hosted by NSWD mergers to satisfy the properties of host galaxies of FRB 180924-like bursts. Thanks to the large range in local environments and host galaxies, however, this channel can also account for the properties of local environment and host galaxy of FRB 180916.J0158+65, i.e., this FRB locates at a star-forming region in a massive spiral galaxy (Marcote et al. 2020).

(7) *Event Rate.* The volumetric event rate of NSWD mergers is in a range of (0.5–1) $\times 10^4$ Gpc^{-3} yr^{-1} in the local universe, which is $\sim$2.5 $\times 10^3$–1 $\times 10^4$ times more than that of the observed LGRBs (Thompson et al. 2009) but roughly lower than that of FRBs by one order of magnitude (Nicholl et al. 2017). Khokhriakova & Popov (2019) obtained a roughly consistent result that the total rate of NSWD mergers is $\sim$850 sky^{-1} day^{-1} using cosmic star formation history from Madau & Dickinson (2014), which is approximately lower than the rate of FRBs $\sim$10$^{3-4}$ sky^{-1} day^{-1} (Cordes & Chatterjee 2019) by one order of magnitude. However, the fraction of NSWD mergers generating magnetars is very unclear. If this fraction is comparable to that of BNS mergers, i.e., 3%, as estimated in Nicholl et al. (2017), the rate of magnetars formed from NSWD mergers is approximately 150–300 Gpc^{-3}yr^{-1} which is comparable to the overall rate of millisecond magnetars born in SLSNe/LGRBs and SGRBs—BNS channels, i.e., few 10–100 Gpc^{-3} yr^{-1} in Nicholl et al. (2017). If this is the case, magnetars formed from the NSWD channel can contribute to at least a subset of FRB 180924-like bursts. Due to a large uncertainty of the magnetar formation rate in the NSWD channel, magnetars formed from this channel are also required to emit several bursts over their lifetimes, especially their active lifetimes, if all of FRB 180924-like bursts result from magnetars, based on Ravi (2019).

4. Summary and Discussion

Assuming there are two FRB populations: FRB 121102-like bursts arise from magnetars born in SLSNe/LGRBs channels while FRB 180924-like bursts arise from magnetars born in BNS/BWD/AIC channels, we have investigated whether FRB 180924-like bursts could also arise from magnetars formed from the NSWD channel, i.e., (1) whether magnetars can be formed from NSWD mergers with unstable mass transfer, and (2) if they can indeed, whether flaring magnetars formed from this channel can explain the observations of FRB 180924-like bursts such as their own characteristics, local environments, host galaxies, and event rates. We explored the first question and speculated that there are two possible scenarios to produce strongly magnetized "renascent" NSs from NSWD mergers. The first scenario is magnetic field amplification by a vigorous α–ω dynamo acting on the accreting NS surrounded by a massive extended hot disk composed of WD debris during the mass transfer process. We performed a preliminary calculation and showed that the magnetic field of the final NS could be enhanced via the dynamo induced by differential rotation and convection in/on the accreting NS, as well as the MRI in the disk. The second scenario is magnetic flux conservation of a fossil field. This scenario could contribute to a small fraction of NSWD binaries in which the NSs are strongly magnetized and remain their magnetic fields before coalescence. Whether or not these scenarios can give rise to magnetars post NSWD mergers still requires evidence from both numerical simulations and observations. As a result, the magnetic field evolution of the remnants requires some deep and complex exploration and magnetohydrodynamics simulations.

In any case, if the NSWD channel can create magnetars, it could produce FRB 180924-like bursts and account for their properties over an active lifetime, burst transparency, circumburst DM, RM, persistent radio source, host galaxy, and event rate within the framework of flaring magnetars because the ejecta, local environments, and host galaxies of the final remnants from this channel resemble those of BNS/BWD/AIC channels. Otherwise, within a large range in local environment and host galaxy, this channel can also account for the observational properties of FRB 180916.J0158+65 (Marcote et al. 2020): not only its properties similar to FRB 180924 such as circumburst DM, RM, and persistent radio source because of the similar ejecta, but also its local environment and host galaxy differing from FRB 180924.

In the future, an evident association between FRBs and magnetars formed from NSWD mergers should need an association of transients most similar to faint type Ib Ca-rich SNe (Metzger 2012) or SNe Ic (Zenati et al. 2019), gravitational waves from NSWD during the inspiral and merger phase detected by eLISA or even aLIGO/Virgo (Paschalidis et al. 2009), and FRBs, if such bursts are indeed produced from flaring magnetars.

ORCID iDs

Shu-Qing Zhong ● https://orcid.org/0000-0002-1766-6947
Zi-Gao Dai ● https://orcid.org/0000-0002-7835-8585

References

Balbus, S. A., & Hawley, J. F. 1998, RvMP, 70, 1
Bannister, K. W., Deller, A. T., Phillips, C., et al. 2019, Sci, 365, 565
Belczynski, K., Kalogera, V., & Bulik, T. 2002, ApJ, 572, 407
Belczynski, K., Perna, R., Bulik, T., et al. 2006, ApJ, 648, 1110
Beloborodov, A. M. 2017, ApJL, 843, L26
Beloborodov, A. M. 2019, arXiv:1908.07743
Beloborodov, A. M., & Li, X. 2016, ApJ, 833, 261
Blackman, E. G., Frank, A., & Welch, C. 2001, ApJ, 546, 288
Bobrick, A., Davies, M. B., & Church, R. P. 2017, MNRAS, 467, 3556
Champion, D. J., Petroff, E., Kramer, M., et al. 2016, MNRAS, 460, L30
Chatterjee, S., Law, C. J., Wharton, R. S., et al. 2017, Natur, 541, 58
CHIME/FRB Collaboration, Amiri, M., Bandura, K., et al. 2019a, Natur, 566, 235
CHIME/FRB Collaboration, Andersen, B. C., Bandura, K., et al. 2019b, ApJL, 885, L24
CHIME/FRB Collaboration, Fonseca, E., Andersen, B. C., et al. 2020, ApJL, 891, L6
Cordes, J. M., & Chatterjee, S. 2019, ARA&A, 57, 417
Cowperthwaite, P. S., Berger, E., Villar, V. A., et al. 2017, ApJL, 848, L17
Cumming, A., Arras, P., & Zweibel, E. 2004, ApJ, 609, 999
Dai, Z. G., Wang, J. S., Wu, X. F., & Huang, Y. F. 2016, ApJ, 829, 27
Dai, Z. G., Wang, X. Y., Wu, X. F., & Zhang, B. 2006, Sci, 311, 1127
Deng, C.-M., Cai, Y., Wu, X.-F., & Liang, E.-W. 2018, PhRvD, 98, 123016
Duncan, R. C., & Thompson, C. 1992, ApJL, 392, L9
Falcke, H., & Rezzolla, L. 2014, A&A, 562, A137
Farah, W., Flynn, C., Bailes, M., et al. 2018, MNRAS, 478, 1209
Fernández, R., Margalit, B., & Metzger, B. 2019, MNRAS, 488, 259
Ferrario, L., & Wickramasinghe, D. 2006, MNRAS, 367, 1323
Ferrario, L., & Wickramasinghe, D. 2008, MNRAS, 389, L66
Frank, J., King, A., & Raine, D. 1992, Accretion Power in Astrophysics, Vol. 21 (Cambridge: Cambridge Univ. Press)
Geng, J. J., & Huang, Y. F. 2015, ApJ, 809, 24
Giacomazzo, B., & Perna, R. 2013, ApJL, 771, L26
Goldreich, P., & Reisenegger, A. 1992, ApJ, 395, 250
Gu, W.-M., Dong, Y.-Z., Liu, T., Ma, R., & Wang, J. 2016, ApJL, 823, L28
Harding, A. K., & Lai, D. 2006, RPPh, 69, 2631
Hessels, J. W. T., Spitler, L. G., Seymour, A. D., et al. 2019, ApJL, 876, L23
Heyl, J. S., & Kulkarni, S. R. 1998, ApJL, 506, L61
Hjellming, M. S., & Webbink, R. F. 1987, ApJ, 318, 794
Hurley, J. R., Tout, C. A., & Pols, O. R. 2002, MNRAS, 329, 897
Kasen, D., Metzger, B., Barnes, J., Quataert, E., & Ramirez-Ruiz, E. 2017, Natur, 551, 80
Kashiyama, K., Ioka, K., & Mészáros, P. 2013, ApJL, 776, L39
Kasliwal, M. M., Kulkarni, S. R., Gal-Yam, A., et al. 2012, ApJ, 755, 161
Katz, J. I. 2016, ApJ, 826, 226
Katz, J. I. 2018, PrPNP, 103, 1
Keane, E. F., Stappers, B. W., Kramer, M., & Lyne, A. G. 2012, MNRAS, 425, L71
Khokhriakova, A. D., & Popov, S. B. 2019, JHEAp, 24, 1
King, A. R., Pringle, J. E., & Wickramasinghe, D. T. 2001, MNRAS, 320, L45
Konar, S., & Bhattacharya, D. 1997, MNRAS, 284, 311
Kumar, P., Lu, W., & Bhattacharya, M. 2017, MNRAS, 468, 2726
Kumar, P., Shannon, R. M., Osłowski, S., et al. 2019, ApJL, 887, L30
Lattimer, J. M., & Prakash, M. 2004, Sci, 304, 536
Liu, X. 2018, Ap&SS, 363, 242
Liu, X. 2020, IJAA, 10, 28
Lorimer, D. R., Bailes, M., McLaughlin, M. A., Narkevic, D. J., & Crawford, F. 2007, Sci, 318, 777
Lu, W., & Kumar, P. 2018, MNRAS, 477, 2470
Lyman, J. D., James, P. A., Perets, H. B., et al. 2013, MNRAS, 434, 527
Lyubarsky, Y. 2014, MNRAS, 442, L9
Lyutikov, M., Burzawa, L., & Popov, S. B. 2016, MNRAS, 462, 941
Madau, P., & Dickinson, M. 2014, ARA&A, 52, 415
Marcote, B., Nimmo, K., Hessels, J. W. T., et al. 2020, Natur, 577, 190
Margalit, B., Berger, E., & Metzger, B. D. 2019, ApJ, 886, 110
Margalit, B., & Metzger, B. D. 2016, MNRAS, 461, 1154
Margalit, B., & Metzger, B. D. 2017, MNRAS, 465, 2790
Margalit, B., & Metzger, B. D. 2018, ApJL, 868, L4

Margalit, B., Metzger, B. D., Berger, E., et al. 2018, MNRAS, 481, 2407
Metzger, B. D. 2012, MNRAS, 419, 827
Metzger, B. D., Beniamini, P., & Giannios, D. 2018, ApJ, 857, 95
Metzger, B. D., Berger, E., & Margalit, B. 2017, ApJ, 841, 14
Metzger, B. D., Margalit, B., & Sironi, L. 2019, MNRAS, 485, 4091
Michilli, D., Seymour, A., Hessels, J. W. T., et al. 2018, Natur, 553, 182
Murase, K., Kashiyama, K., & Mészáros, P. 2016, MNRAS, 461, 1498
Nicholl, M., Williams, P. K. G., Berger, E., et al. 2017, ApJ, 843, 84
Nomoto, K., & Kondo, Y. 1991, ApJL, 367, L19
Nordhaus, J., Wellons, S., Spiegel, D. S., Metzger, B. D., & Blackman, E. G.
    2011, PNAS, 108, 3135
Parfrey, K., Spitkovsky, A., & Beloborodov, A. M. 2016, ApJ, 822, 33
Paschalidis, V., Etienne, Z., Liu, Y. T., & Shapiro, S. L. 2011a, PhRvD, 83,
    064002
Paschalidis, V., Liu, Y. T., Etienne, Z., & Shapiro, S. L. 2011b, PhRvD, 84,
    104032
Paschalidis, V., MacLeod, M., Baumgarte, T. W., & Shapiro, S. L. 2009,
    PhRvD, 80, 024006
Perets, H. B., Gal-Yam, A., Mazzali, P. A., et al. 2010, Natur, 465, 322
Petroff, E., Barr, E. D., Jameson, A., et al. 2016, PASA, 33, e045
Petroff, E., Hessels, J. W. T., & Lorimer, D. R. 2019, A&ARv, 27, 4
Piro, A. L., & Burke-Spolaor, S. 2017, ApJL, 841, L30
Piro, A. L., & Ott, C. D. 2011, ApJ, 736, 108
Platts, E., Weltman, A., Walters, A., et al. 2019, PhR, 821, 1
Popov, S. B., Postnov, K. A., & Pshirkov, M. S. 2018, PhyU, 61, 965
Price, D. J., & Rosswog, S. 2006, Sci, 312, 719
Prochaska, J. X., Macquart, J.-P., McQuinn, M., et al. 2019, Sci, 366, 231
Quataert, E., & Gruzinov, A. 2000, ApJ, 539, 809
Ravi, V. 2019, NatAs, 3, 928
Ravi, V., Catha, M., D'Addario, L., et al. 2019, Natur, 572, 352
Rosswog, S., Ramirez-Ruiz, E., & Davies, M. B. 2003, MNRAS, 345, 1077
Schwab, J., Quataert, E., & Bildsten, L. 2015, MNRAS, 453, 1910
Schwab, J., Quataert, E., & Kasen, D. 2016, MNRAS, 463, 3461
Spitler, L. G., Scholz, P., Hessels, J. W. T., et al. 2016, Natur, 531, 202
Sun, S., Li, L., Liu, H., et al. 2019, PASA, 36, e005
Tauris, T. M., Sanyal, D., Yoon, S. C., & Langer, N. 2013, A&A, 558,
    A39
Tendulkar, S. P., Bassa, C. G., Cordes, J. M., et al. 2017, ApJL, 834, L7
Thompson, C., & Duncan, R. C. 1993, ApJ, 408, 194
Thompson, C., & Duncan, R. C. 1996, ApJ, 473, 322
Thompson, T. A., Kistler, M. D., & Stanek, K. Z. 2009, arXiv:0912.0009
Thorne, K. S., & Zytkow, A. N. 1977, ApJ, 212, 832
Thornton, D., Stappers, B., Bailes, M., et al. 2013, Sci, 341, 53
Toonen, S., Perets, H. B., Igoshev, A. P., Michaely, E., & Zenati, Y. 2018,
    A&A, 619, A53
Tout, C. A., Wickramasinghe, D. T., Liebert, J., Ferrario, L., & Pringle, J. E.
    2008, MNRAS, 387, 897
Troja, E., Rosswog, S., & Gehrels, N. 2010, ApJ, 723, 1711
Turolla, R., Zane, S., & Watts, A. L. 2015, RPPh, 78, 116901
Urpin, V., & Konenkov, D. 1997, MNRAS, 284, 741
van Haaften, L. M., Nelemans, G., Voss, R., Wood, M. A., & Kuijpers, J.
    2012, A&A, 537, A104
Villar, V. A., Guillochon, J., Berger, E., et al. 2017, ApJL, 851, L21
Wang, J.-S., Yang, Y.-P., Wu, X.-F., Dai, Z.-G., & Wang, F.-Y. 2016, ApJL,
    822, L7
Xue, Y. Q., Zheng, X. C., Li, Y., et al. 2019, Natur, 568, 198
Yoon, S. C., Podsiadlowski, P., & Rosswog, S. 2007, MNRAS, 380, 933
Zenati, Y., Bobrick, A., & Perets, H. B. 2020, MNRAS, 493, 3956
Zenati, Y., Perets, H. B., & Toonen, S. 2019, MNRAS, 486, 1805
Zhang, B. 2014, ApJL, 780, L21
Zhang, B. 2016, ApJL, 827, L31
Zhang, B. 2017, ApJL, 836, L32
Zhang, B. 2018, ApJL, 867, L21
Zhong, S.-Q., Dai, Z.-G., & Li, X.-D. 2019, PhRvD, 100, 123014